Landscape Ecology vol. 2 no. 1 pp 3-22 (1988)
SPB Academic Publishing, The Hague

Linking knowledge among spatial and temporal scales: Vegetation, atmosphere, climate and remote sensing

Forrest G. Hall, Donald E. Strebel, and Piers J. Sellers
*Goddard Space Flight Center, **NASA,** Greenbelt, Maryland 20771, USA*

Keywords: global models, atmosphere, climate, remote sensing, FIFE, biosphere

Abstract

Global scale modeling is reviewed with respect to global circulation models, biosphere-atmosphere models, and climate-biosphere models. These different models focus on short to long time scale interactions between atmospheric and surface systems. Remote sensing is shown to play a central role in acquisition of data for these models, and an experiment, termed FIFE, is described, which is the first attempt to take simultaneous land surface observations of meteorological and biophysical parameters at sufficient resolution to test hypotheses linking the vegetated surface and circulation within the lower atmosphere.

Introduction

Advances in the earth sciences in recent years have resulted in a growing body of knowledge concerning the interactions between the earth's biosphere, oceans, ice and atmosphere and have shown that there are couplings of varying strength between these systems over a wide range of temporal and spatial scales. For example, agricultural and industrial activities that modify terrestrial vegetation and atmospheric trace gas composition have been hypothesized to have global effects on the climate and the composition of terrestrial ecosystems within the next few decades (see the review of MacCracken and Luther 1985). Thus we critically need to better understand the interactions among the earth's coupled systems, and in particular, the effects of anthropogenic activities.

We illustrate some of the problems involved in understanding and modeling phenomena operating at a variety of spatial and temporal scales across regional and global landscapes and indicate how satellite remote sensing data can play a role in transferring information from one scale domain to another. We also suggest a strategy for future experimentation, involving a multi-disciplinary effort to simultaneously study the interactions between the terrestrial surface and the atmosphere and the interactions between the climate and terrestrial ecosystems. Finally, we discuss the rationale, design and some early results from (1) the First ISLSCP (International Satellite Land Surface Climatology Project) Field Experiment (FIFE), an intensive study of the interactions between land surface vegetation and the atmosphere (Sellers *et al.* 1988), and (ii) a forest dynamics modeling effort (Hall *et al.* 1986) aimed at constructing regional scale models of forest landscape dynamics.

Coupling between the terrestrial biosphere and atmosphere occurs across a wide range of temporal and spatial scales. In the simplified diagram of Fig. 1, (which ignores the interactions with the oceans and continental ice) three coupled feed-back loops are shown. A strong, fast-response feed-back loop

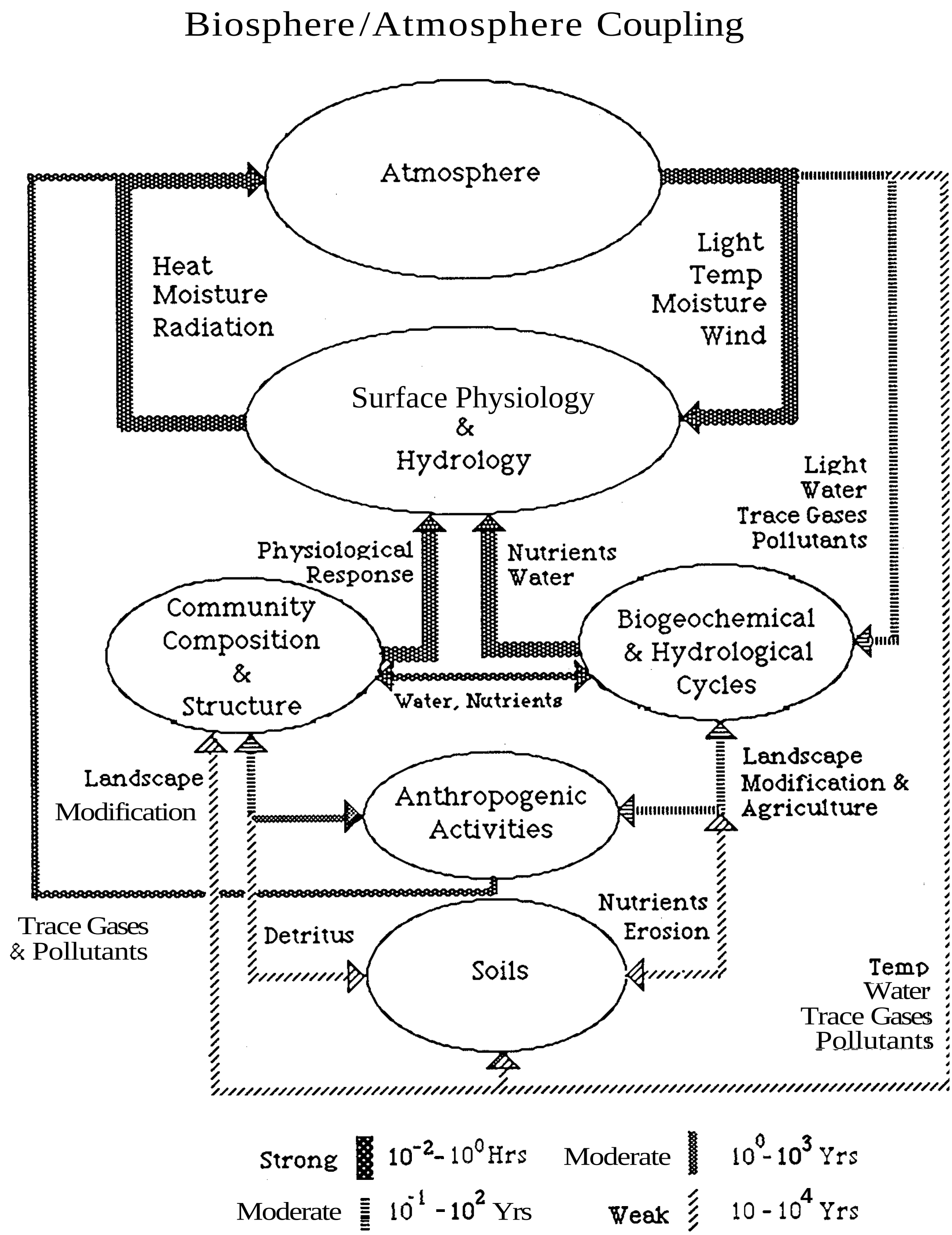

Fig. 1. Major elements in the coupling among the atmosphere and terrestrial ecosystems. This simplified diagram emphasizes the time scales involved in the various couplings. The lower atmosphere and surface vegetation are coupled with a fast-response loop through the partitioning of incident solar radiation at the land surface and subsequent circulation of moisture and heat in the lower atmosphere which affects the physiology of the surface vegetation. The atmosphere is also coupled through weaker responses at longer time scales by climate modifications to biogeochemical and hydrological cycles, soils and community composition and structure.

(minutes to hours) couples the physiological status of the terrestrial vegetation (photosynthetic and evapotranspiration rates) to the atmospheric state. The atmospheric state (net radiation at the surface, precipitation, temperature and humidity) in turn modifies the photosynthetic and transpiration rates of the surface vegetation on a similar time scale. A weaker, slower feed-back loop (months to centuries) couples the atmosphere (climate) to terrestrial biogeochemical and hydrological cycles and vegetation structure (phenology, height, condition, etc.). A third, even weaker, feed-back loop (decades to millenia) couples the climate to the community composition and structure of the terrestrial landscape and the underlying soils. Of key interest is the effect of anthropogenic activities, which can couple strongly to and rapidly modify any one of the above systems.

Because these feed-back loops operate at such diverse time and space scales, modeling of these systems can be accomplished to some degree by assuming that the systems are decoupled. For example, computer simulations of future (or past) climate assume a constant terrestrial landscape. Such an assumption might be reasonable for periods of time shorter than that required for the landscape to respond significantly to climate. Conversely, computer-simulated projections of landscape dynamics can use as input a climate scenario generated by an atmospheric simulation decoupled from the landscape structure. This assumption might be reasonable for inconsequential changes in the landscape structure. However, for investigations of phenomena acting over periods of time large in comparison to the scales at which these systems couple, the interactions among the systems must be considered. When they are, positive or negative feedback can result in solutions very different from the decoupled solutions. These are the kinds of solutions which are of interest in projecting the impact of anthropogenic and other effects on the future status of the climate and terrestrial biota over time scales of decades to centuries.

In the following, we review very briefly the status of global scale modeling in the context of Fig. 1; first with regard to atmospheric global circulation models (GCMs), then biosphere-atmosphere models, which describe the short-time scale interactions between the land surface and atmosphere, and finally the climate-biosphere models, which describe the longer time scale interactions between the climate, humans and the biosphere.

Atmosphere-biosphere models in GCMs

The last forty years have seen rapid development in the area of weather and climate simulation. The main tool for this work is the GCM which is essentially a computer program that integrates the governing equations for the atmosphere over short time steps to produce a semi-continuous picture of the changing planetary circulation. The equations that determine the time-evolution of the atmosphere can be broadly lumped into two components; fluid dynamics equations which describe the motion of the atmosphere and the physics equation set, which describes the effects of heating, friction and turbulence on the atmosphere. Solution of this complex, non-linear system of equations can only be achieved numerically. Thus, in a GCM, the globe is partitioned into grid squares and the overlaying atmosphere into several layers. The equation set is then solved numerically over the grid and the future state of the atmosphere (at each grid cell) is computed. Successive integrations have the effect of simulating the dynamic atmosphere circulation.

GCM’s have been improved over the last three decades to the point where they are routinely applied for weather forecasting and climate simulation. The advent of large, efficient computers and the development of efficient computational schemes, see Orszag (1970), Sela (1980), Arakawa and Suarez (1983), have resulted in the development of realistic models of atmospheric dynamical processes at high temporal (12 to 30 minutes) and spatial (1° to 5° longitude/latitude) resolution. As the mathematical representation of the fluid dynamics of the atmosphere improved, focus in model development shifted to upgrading the description of physical processes (radiational heating, turbulent transport, friction, latent and sensible heating) and initialization schemes in the GCM's. According to Wiin-Nielsen (1976), the contributions to total error in numerical weather prediction for a series of short range forecasts were as follows: total truncation error, *i.e.*, error in the dynamics description, 48%; errors in the initial condition specification, 18%; and errors in the physics 34%. These errors were calculated from a number of two-day forecasts; it is expected that for longer simulations, the errors due to shortcomings in GCM physical descriptions would take a dominant role.

One set of physical processes was largely neglected until the early 1980's; that of the land surface-atmosphere interaction. Prior to the work of Dickinson (1984), almost all GCM's parameterized the exchange of radiation and momentum between the land and atmosphere by independently specifying fields of surface albedo and roughness length over the Earth's surface. The net radiation at the surface could then be simply calculated by

$$R_n = S(1-\alpha) + L_{wd} - \epsilon\sigma T_s^4 \tag{1}$$

R_n = net radiation, Wm^{-2}
S = total solar radiation incident on the surface Wm^{-2}
α = broad-band surface albedo
L_{wd} = downwelling long wave radiation, Wm^{-2}
T_s = surface temperature, K
ϵ = surface emissivity
σ = Stefan-Boltzman constant, $J\ m^{-2}\ K^{-4}$

Shear stress exerted on the atmosphere by the surface was calculated as

$$\tau = \rho\ u_r/r_{am} \tag{2}$$

τ = shear stress, $kg\ m^{-1}\ s^{-2}$
ρ = density of air, $kg\ m^{-3}$
u_r = wind speed at a reference height above the surface, $m\ s^{-1}$
r_{am} = aerodynamic resistance for momentum transfer, $s\ m^{-1}$

τ results in a transfer of momentum from the atmosphere to the surface by decelerating a parcel of air moving horizontally at the surface. τ is proportional to the difference between the unperturbed wind speed, u_r, and the wind speed u_o at the surface (assumed in (2) to be zero) and inversely proportional to an aerodynamic resistance r_{am} which regulates the momentum flux. r_{am} is conventionally calculated using an eddy diffusion concept, whereby a 'conductance' to momentum transfer is inverted and integrated between the surface and the reference height. Under neutral conditions, r_{am} is given as,

$$r_{am} = 1/u_r[1/k\ \ln\ (z_r/z_o)] \tag{3}$$

k = von Karman's constant, 0.41
z_o = roughness length, m
z_r = reference height, m

The roughness length z_o in **(3)** is a function of the height and density of the surface vegetation. This means that rough surfaces, *e.g.*, forests and shrublands are more strongly coupled to the atmosphere via turbulent transfer than are smooth surfaces such as deserts and grasslands.

The net radiation R_n, as given by (1), from the surface to the atmosphere is partitioned into three components at the earth's surface, *i.e.*,

$$R_n = H + \lambda E + G \tag{4}$$

H = sensible heat flux (conduction to the air), Wm^{-2}
λE = latent heat flux (release to the air by evaporation), $W\ m^{-2}$
h = heat of vaporization, $J\ kg^{-1}$
E = moisture flux into the air, $kg\ m^{-2}\ s^{-1}$
G = heat flux into the ground, $W\ m^{-2}$

On land surfaces, the magnitude of each component is determined by the community composition and structure of the surface vegetation, its reflective properties, its rate of photosynthesis and transpiration (water loss) and the water storage and loss characteristics of the underlying terrain and soils. **As** measurements by Asrar and Kanemasu (1986) show for the grasslands of central Kansas (Fig. 2), the magnitudes and components of the budget vary with time and terrain.

Over a day or longer, the ground heat flux G averages out to be a relatively small term, seldom more than about 10% of R_n. H and λE are much larger and the magnitude of the ratio of sensible to latent heat release into the atmosphere (the Bowen

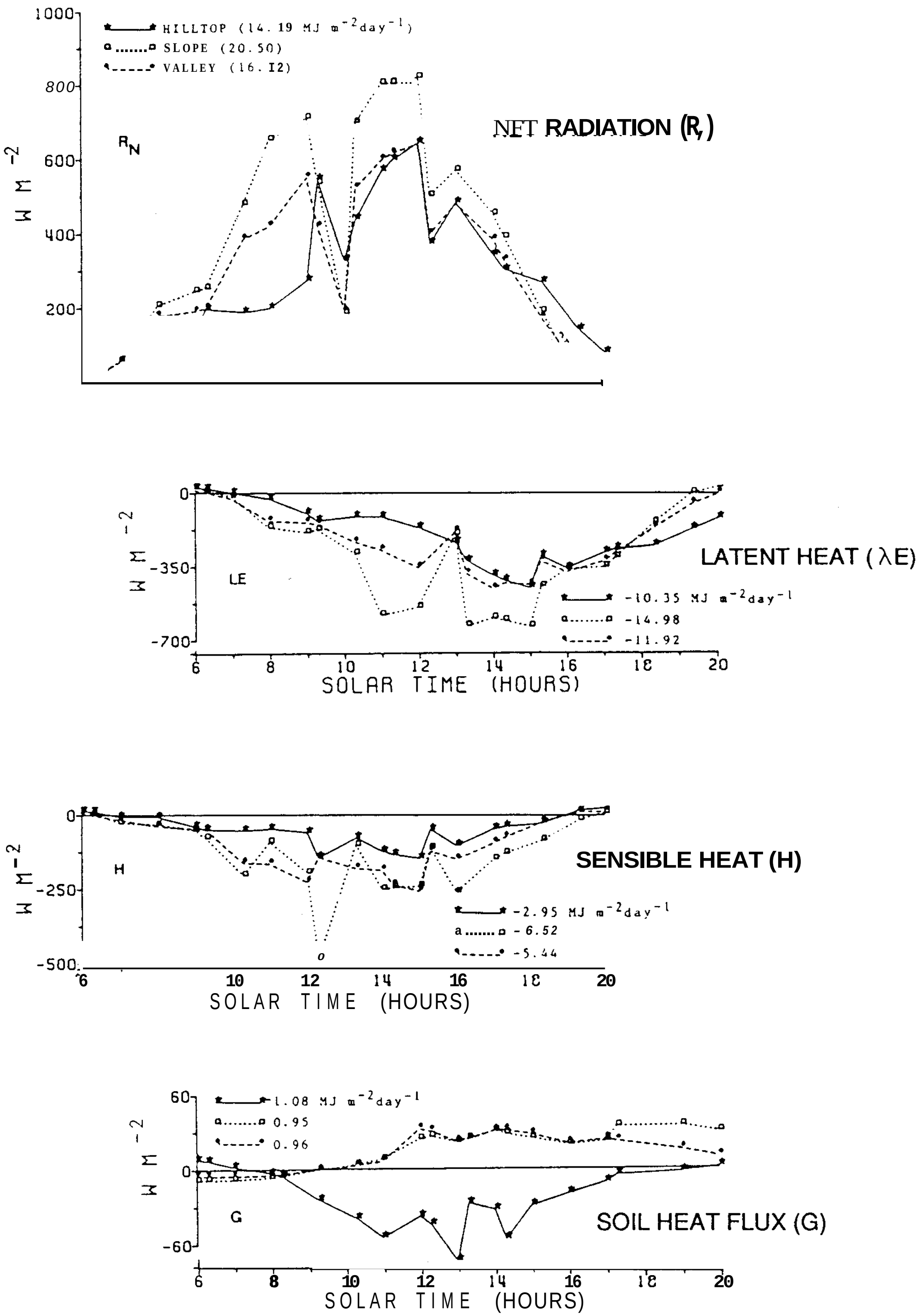

Fig. 2. Components of the radiation budget in a tall grass prairie, July 20th, 1985 for a hilltop, a west-facing slope and a valley bottom. Slope determines soil depth, root-zone soil moisture available for latent heating. Note decrease in latent and sensible heat **flux** following the decrease in solar radiation beginning at 12:00 noon.

ratio) can be an important determinant of the local and regional climate. Sensible heat flux heats the air above the surface locally in both space and time – its major effect is to provide a forcing for the development of the planetary boundary layer (PBL) in the daytime hours. The latent heat flux may have a small local heating effect, but generally the released water vapor is transported into the free atmosphere, moved downstream by the winds and condenses to form clouds and precipitation some distance in time and space from its point of release. Since these two modes of heat release have such different effects on the internal heating radiative properties of the atmosphere (condensing water vapor forms clouds), the accurate calculation of the terms in the surface energy budget (4) is of real importance to the realistic prediction of atmospheric circulation.

A key assumption to the calculation of the surface energy budget is the biology and mechanics of moisture storage and release by vegetation and soils. Prior to the mid-1980's the Budyko bucket model was used in almost all GCM's to calculate the storage and release of moisture (see the reviews of Carson 1981, and Mintz 1984). Generally, the bucket model specifies a maximum water holding capacity (usually taken to be 15 cm) for each grid area within the GCM. The actual volume of water in the bucket is determined by the time series of precipitation (addition) and evaporation (subtraction). The surface energy balance is then calculated by

$$G = f\,(dT_s/dT) \tag{5}$$

$$H = (T_s - T_a)\,\rho C_p/r_a \tag{6}$$

$$\lambda E = \beta(\rho C_p/\gamma)\,[e_*(T_s) - e_a]/r_a \tag{7}$$

T_a, e_a = air temperature and vapor pressure, K, mb

$e_*(T_s)$ = saturated vapor pressure in the canopy air space at surface temperature, mb

γ = psychrometric constant, mb K^{-1}

β = moisture availability function

r_a = aerodynamic resistance for heat and water vapor, s m^{-1}

z = depth below surface, m

In (5) G is calculated using models of soil conduction which vary in complexity and realism (see Deardorf 1977). In (6) and (7) the aerodynamic resistance, r_a, is calculated in much the same way as r_{am} is in (2), with a similar dependence on z_o. The most important determinant of the energy budget in this formulation is β, the moisture availability function. In most GCM's this is taken as a simple monotonic function of the level of water in the bucket, *i.e.*,

$$\beta = f(S/S_{max}) \tag{8}$$

for example $\beta = 4/3\ (S/S_{max}),\ 0 < \beta < 1$

S = bucket water level, mm, S_{max} = maximum value of S, usually 15 cm.

The example given above is used in a number of GCM's, including the National Meteorological Center model for medium range forecasts and a number of climate simulation models, see Miyakoda and Sirutis (1986).

These simple models of land-surface atmosphere interactions have been used extensively in studies which have investigated the sensitivity of the atmospheric motion, precipitation, temperature and humidity fields to changes in the bulk land surface parameters of albedo, roughness length and surface wetness. For example, Charney *et al.* (1977) executed a series of GCM sensitivity experiments examining the effects of surface albedo change in the Sahel, which indicated that an increase in the albedo of the region would lead to a decrease in the surface evaporation rate and a reduction in the precipitation rate in the same area. This study has been followed by similar ones on the Sahel/Sahara area (Sud and Fennessy 1982) and Chervin (1979) which produced the same result qualitatively if not quantitatively. Carson and Sangster (1981) performed a more radical experiment by comparing simulation runs performed with GCM's wherein the albedo of the global land surface was prescribed as being 0.1 or 0.3. The higher albedo case was associated with a reduction in the continental precipitation rate from 4.6 mm/day to 3.4 mm/day which roughly corresponded with the reduced land surface evaporation, 3.7 mm/day to 2.7 mm/day for the higher albedo case. *In situ* observations indicate that the land surface albedo varies from about 0.12 for tropical rain forest to 0.35 for the Sahara desert (see Shuttleworth et al. 1984 and Matthews 1983).

The effect of changing surface roughness length (z_o) was investigated in a study by Sud and Smith (1985): the roughness length of the world's deserts was drastically reduced from 45 cm to 0.2 mm which brought about changes in the fields of horizontal water vapor convergence and associated changes in the distribution of convective precipitation.

Not surprisingly, many sensitivity studies have been devoted to investigating the role of land surface hydrology in the exchange of energy between the surface and atmosphere. Walker and Rowntree (1977), Carson and Sangster (1981), Shukla and Mintz (1982), Warrilow (1986) and others reviewed in Mintz (1984) have performed experiments ranging from global prescriptions of totally wet versus totally dry land surfaces to alterations in regional soil moisture capacities. In almost all cases, reduced land surface evaporation rates led to reduced precipitation in continental interiors.

These experiments served to demonstrate that the specification of albedo, roughness and perhaps, most importantly, the 'surface wetness' could have important impacts on the atmospheric fields of temperature, precipitation, wind speed and humidity. It was first pointed out by Dickinson (1984) that these experiments, though illustrative, were unrealistic, particularly with regard to the description of the land surface evapotranspiration process as conventionally specified by the bucket model in the GCM's. He proposed that more realistic descriptions of land surface processes be incorporated with GCM's and designed such a model which attempts explicitly to account for the effects of vegetation.

The particular problem with the commonly used bucket hydrology formulation in **(7)** is that it is a poor representation of the evapotranspiration process as it occurs in nature, where the plant canopy stomatal resistance exerts a powerful role in regulating the transfer of water from soil to atmosphere. **A** more realistic description of the evapotranspiration rate as forwarded by Monteith (1973), is

$$\lambda E = (\rho C_p/\gamma)\,[e_*(T_S) - e_a]/[r_a + r_{surf}] \qquad (9)$$

r_{surf} = bulk surface (soil and canopy) resistance, s m^{-1}.

Here, as opposed to (8), the role of vegetation is explicitly acknowledged in the r_{surf} term which parameterizes the resistance of vegetation and soil to moisture transpiration and evaporation from the surface (and is often dominated by the vegetation stomatal resistance).

The models of Dickinson (1984) and the Simple Biosphere model (SiB) of Sellers et al. (1986) use different manifestations of (9) in their evapotranspiration formulation. In particular, SiB attempts to model the vegetation inself, and thereby calculate mutually consistent values of albedo, surface roughness and surface (stomatal) resistance. Preliminary results from the models of Dickinson (1986) and Sellers et al. (1986), indicate that the 'realistic' vegetation models generate far less evaporation over the continents than the conventional abiotic bucket models. This has had the effect of reducing continental precipitation rates, particularly in the northern hemisphere summer, increasing the daytime PBL heights and increasing the diurnal amplitude of the near-surface air temperature wave. All of these effects have brought GCM simulations into closer agreement with observations which indicates that the realistic modeling of vegetation should yield practical dividends in improved weather forecasts as well as better climate simulations for scientific research.

The role of remote sensing in vegetation-atmosphere interactions

The vegetation-atmosphere models of Sellers et al. (1986) and Dickinson (1984) are based on our current understanding of biological processes on the scale of individual plants and small plots. Remote sensing has a central role to play in the acquisition of data at synoptic scales and high time resolution; this will allow us to integrate our understanding of small scale processes up to the larger (regional) scales appropriate to understanding the coupling between the terrestrial landscape and the atmosphere. It is essential that we learn how to do this if we wish to estimate the parameters (albedo, roughness length, surface resistance) of the vegetation-atmosphere interaction models and initialize the model's prognostic variables (*e.g.*, soil moisture or initial evapotranspiration rate) at large spatial scales, *i.e.*, regional, continental, global.

Theory and experiment have indicated that it is possible to estimate some of the above quantities from remotely sensed data; specifically, the components of the radiation budget, the roughness length, the surface resistance and soil moisture.

Radiation budget. Different components of the surface radiation budget can be estimated from satellite data, for example measurements of radiance from the surface can be used to estimate surface albedo, and insolation. Thermal and microwave instruments may be used to estimate the upwelling longwave radiation, $\epsilon\sigma T_s^4$ in (1) and the surface temperature itself. Given that we can estimate L, and $\epsilon\sigma T_s^4$ from satellite data it is feasible to calculate the surface net radiation R, from (1). These satellites include the NOAA polar orbiters, the geosynchronous GOES satellites, Landsat and SPOT. Sounding instruments on the NOAA polar orbiters may be used in conjunction with a considerable modeling effort to estimate the downwelling radiation L, of (1). It should be pointed out that the extraction of these parameters from the satellite observed radiances (at the top of the atmosphere) is not straightforward given problems of viewing geometry, sensor calibrations, narrow-band to broad-band interpolation, cloud screening and atmospheric corrections. However, a number of algorithms exist to compensate for these effects, and research continues to improve them.

Surface roughness. The sensitivity studies of Sud and Smith (1985) and Sellers and Dorman (1987) indicate that the climate system is relatively insensitive to uncertainties in the surface roughness field. The use of remotely sensed data to classify the earth's surface into vegetation categories, combined with morphological data for each category, can potentially provide estimates of the roughness length (z,) field. The effect of surface roughness on the backscatter of coherent and incoherent microwave radiation (measureable with radar and passive microwave instruments) has been investigated both experimentally and through the development of theoretical models (Fung and Eom 1981; Tsang *et al.* 1982, 1986; Mo *et al.* 1984; Pitts *et al.* 1987, 1988). These studies develop models that relate the morphological characteristics of vegetated canopies to the strength of the scattered microwave signal. By using these models and inversion techniques it may be possible to utilize measured radar back scattering cross section to extract vegetation canopy morphological properties (*e.g.*, canopy height and density) for use in (2) and (5).

Surface resistance and soil moisture. Surface resistance and soil moisture determination are bound up with our understanding of how vegetation controls the energy budget. A number of different (though related) methods for extracting these parameters have been proposed; these include analyses of the surface temperature, visible and near-infrared reflectances (the spectral vegetation indices) and the microwave emission from the soil surface.

With regard to surface temperature, satellite observations-of T, may be converted to the 'aerodynamic' surface temperature T, in (6). Meteorological data can be used to estimate r_a and T_a over the site and the sensible heat flux H may be calculated from (6). XE may then be obtained as a residual from (4), provided observations or estimates of R, and G are available.

With regard to spectral vegetation indices, the reflectance of vegetation in the near infrared increases more rapidly with increasing vegetation 'density' than does the visible reflectance (over a limited range of leaf area index and vegetative ground cover). Various spectral vegetation indices (VI) exploit this to achieve an index which increases with increasing vegetation 'density' (*e.g.*, leaf area index or biomass and percent ground cover). Two of the simple VI are given by

$$\text{Simple Ratio (SR) VI} = R_{nir}/R_{vis} \tag{10}$$

$$\text{Normalized Difference (ND) VI} = (R_{nir} - R_{vis})/(R_{nir} + R_{vis})$$

$R_{nir}R_{vis}$ = reflectances, radiances or sensor counts in the near infrared, visible regions, respectively.

A more complex VI, the Kauth-Thomas greeness (Kauth *et al.* 1976), has been developed to be minimally sensitive to brightness variations in the scene resulting from soil background and illumination changes.

Typically, the SR varies from around unity for bare soil and steadily increases with increasing green vegetation density. Sellers (1985) and (1987) and Hope (1987) have explored the theoretical relationships between two of the simpler vegetation indices and area-averaged vegetation physiological properties. There are indications that under some conditions (*e.g.*, homogeneous vegetation canopies) the **SR** varies with the illuminated chlorophyll density in a nearly linear fashion which implies that **SR** may be an indicator of (stress-free) photosynthetic capacity. Since the canopy photosynthetic rate and bulk stomatal resistance are closely coupled to yield an efficient assimilation versus transpiration rate (see Farquhar and Sharkey 1982), it is also postulated that the **SR** may provide an indicator of the minimum bulk stomatal resistance. This term may be used, with modifications for stress, in (9), where the surface resistance r_{surf}, appears as an explicit control on evapotranspiration.

In regard to soil moisture, some vegetation-atmosphere models, including SiB calculate the canopy resistance as a function of plant physiological terms and soil moisture. Solution of the energy balance relations (4) to (9) using remotely sensed data may allow an inference of the soil moisture in the root zone. In addition, microwave remote sensing has shown some promise of measuring the soil moisture in the upper few centimeters of the surface soil layer (see for example, Schmugge 1983; Dobson and Ulaby 1986). These data also have potential when used in conjunction with water and energy balance relations to infer a root zone moisture.

In summary, it is proposed that realistic biophysical models can improve our representation of land surface-atmospheric interactions. It is also apparent that such models are of limited use without the ability to obtain input parameters on a global scale. Obviously, satellite remote sensing is a candidate for obtaining such data. However, many of the hypotheses proposed for obtaining these data using remote sensing have not been fully tested. In addition, few of the land surface-atmospheric interaction models themselves have been tested at scales above the plant or plot level.

FIFE: A test of the biosphere-atmosphere coupling hypotheses and an evaluation of remote sensing

Prior to FIFE, there had been no serious attempt to take simultaneous land surface observations of meteorological and biophysical parameters at sufficient temporal and spatial resolution, over a large enough area to permit a rigorous test of the hypotheses linking the vegetated land surface and circulation within the lower atmosphere or the ability of remote sensing to monitor these processes. In fact, very little work in addressing these issues has been carried out at length scales larger than a few hundred meters.

In 1983 the ISLSCP recognized that such an experiment was urgently necessary and FIFE was proposed as the pioneer effort. In late 1986 and early 1987 an experiment plan was developed by 30 science teams competitively selected to participate in the FIFE over a three-year period (Sellers and Hall 1987). The science teams were multidisciplinary in composition, including atmospheric physicists, hydrologists, plant biologists, ecologists, physicists, and a number of other disciplines. Investigations were funded by NASA, NSF, NOAA, and the USDA, FIFE, as it stood after the first year, has been described by Sellers *et al.* (1988).

In FIFE, investigators were faced with two problems: (i) whether the understanding of biological and thermodynamic processes on the small scale of microns to meters could be integrated over space to describe interactions appropriate to atmospheric length scales and (ii) whether remote sensing could be used, along with ground measurements, to monitor such processes at synoptic scales.

To test these ideas, a 15 by 15 kilometer test site was selected over a rather homogeneous grassland, including the 6 by 6 km Konza Prairie Long Term Ecological Research site near Manhattan, Kansas. The Konza consists entirely of native prairie grasses and is relatively gentle in terrain, with an elevation of ~ ± 50 meters throughout. The area was selected primarily for its relative homogeneity, but also for the ease with which supporting ground and aircraft measurements could be accomplished. The FIFE test area is located near airports and Kansas State University with good laboratory facilities.

An experiment design was developed to simultaneously measure throughout several 24 hour periods during the growing season (i) the mass and energy flux in and out of the FIFE test site (ii) the mass and energy flux as a function of characteristics within the site (iii) the biophysical characteristics of the surface vegetation within the site (iv) narrow-band reflected and emitted short and long-wave radiation at different spatial resolutions and altitudes and (v) atmospheric optical parameters necessary to understand the effects of atmospheric electromagnetic scattering on radiation sensed at satellite altitudes. Diurnal satellite, aircraft and ground measurements of these variables were obtained throughout the growing season (April to October). Ground measurements were acquired at 32 sites within the Konza. A probability sample of sites were placed within strata representing the major spatial variation in soil depth, seasonally integrated incident solar radiation and management practice (*e.g.*, grazing and burning).

To study the biosphere-atmosphere interactions at a variety of scales, the relevant biological and thermodynamic processes were measured at resolutions ranging from individual plant leaves up to the entire 15 by 15 km site. Radiometric data were collected at the leaf (10^{-2} m^2), canopy, (1 m^2) and sample site (10–100 m^2) scales using a variety of truck, aircraft and satellite platforms (Aircraft-mouted Thematic Mapper Simulator- 12 m resolution, SPOT-20 m resolution, Landsat- 30 m resolution, AVHRR-1 km resolution and GOES-1 to 8 km resolution). The rationale for the different platforms was the need to (i) validate a number of hypotheses concerning the scaling of radiometric properties from the leaf to the canopy and community level (ii) investigate the accuracy with which satellite data could be calibrated and corrected for atmospheric interference (iii) ascertain the degree to which the relations (1), (2), (3) and (4) were valid at different spatial scales.

Energy and mass flux data were also collected at the leaf, canopy, sample site and study area scales. Porometers, closed flux meters, Bowen ratio, surface and airborne eddy correlation, SODAR and LIDAR equipment were utilized to perform these tasks. Biophysical data (vegetation, physiological, physical, and optical properties, soil physical and chemical properties, soil moisture, etc.) were also acquired. Here we wanted to test the hypotheses stated in (2) and (4) at the sample plot level where we could precisely measure the various process rates, and more importantly at the 15 km by 15 km level to determine if the hypotheses were scale invariant and if the process rates could be inferred from satellite.

A number of serious technical and operational problems had to be overcome in order to accomplish these objectives. It was not known ***apriori*** if the surface heat, moisture and gas fluxes could be accurately measured in the presence of even the modest heterogeneity of the FIFE test area. Further, the techniques for using aircraft-mounted eddy-correlation instruments to accurately measure area averaged surface fluxes had not been fully developed. Finally, there had never been a sensor calibration and atmospheric correction study of this detail and size. The extreme operational complexity of FIFE resulted from the need to simultaneously acquire these data with a variety of platforms, all to be coordinated with the measurement groups from the 30 FIFE science teams. Several trucks, six aircraft and five satellites had to coordinated to acquire cloud free data for several diurnal cycles.

During the 1987 field effort, most of the FIFE measurement objectives were accomplished. The data are being stored in an information management system at the Goddard Spaceflight Center with access via telephone and high-speed links to all the FIFE investigators. To collect the data, a team of FIFE scientists were in residence at the FIFE site for sixty days throughout the field season, meeting daily to define the mission plan given the forecast weather for the following day. The analysis of the data is in process, will continue over at least the planned three-year life time of FIFE and results will be reported in the scientific literature over the next several years.

Climate-biosphere models

Of the many disciplines where regional and global modeling of ecosystem response to climate is underway, we would like here to focus on the study of regional forest dynamics using satellite remote sensing and forest succession models. Forests are a logical focus because they constitute a major store of live, organic carbon, are very sensitive to climate change and are being rapidly altered by human activities. In addition, efforts over the past few years have produced regional-level forest dynamics and succession models which model forest response to both climate change and human activities. Finally, a number of remote sensing efforts over the past few years have resulted in techniques to monitor forest characteristics at synoptic scales.

Forest dynamics is affected by phenomena operating at many temporal and spatial scales. Temporally, for example, gradual warming since the last ice age has resulted in a retreat northward of the southern boundary of the boreal forest (Solomon and Webb 1985). Anthropogenic effects such as fire suppression during this century have had more immediate effects. Soils and topography affect the pattern and process of terrestrial landscapes at scales of meters to kilometers. Stochastic processes such as death, disease, and variations in canopy light levels, nutrient supply rates, and moisture availability affect growth and competition of individual tree canopies and subsequent succession dynamics at meter scales and below.

Various methods have been pursued to understand the response of forested ecosystems to climate and other factors. One approach involves using tree pollen data from radiocarbon-dated sediments to follow the change of the spatial distribution of plant species over the past 20,000 years. Comparisons of these distributions with paleoclimatic data yield insight as to how communities respond to climate (Solomon and Webb 1985). A second method uses comparisons of current geographic distributions of vegetation to current climate (Emanuel *et al.* 1985) to relate vegetated ecosystem boundaries to broad climatic zones. A third method involves computer simulation models of forest dynamics. The early forest dynamics models (*e.g.*, Botkin 1972) incorporated hypotheses concerning birth, growth and death at the individual plant level. Later models, succession models (Shugart *et al.* 1973; Shugart and West 1980; Shugart 1984), used the growth relations developed by Botkin (1972) to model plant communities at the plot level incorporating additional hypotheses concerning competition for light, water and nutrients. A fourth approach involves the use of statistically based forest dynamics models which define a taxa of ecological states and then assesses the frequency with which transitions are observed from one state to another, over a specified period of time (Horn 1975a, b, 1976). Conceptually, the transition frequencies can be used as inputs for Markov models of succession in the ecosystem. Recent reviews of such models for vegetation dynamics are found in Usher (1981) and Hulst (1979).

To develop, execute and test the forest dynamics models, modelers are restricted to input and output parameters which are practical to measure given available resources and technology. The labor intensive nature of traditional field data collection has severely constrained model development and testing, particularly at the landscape level. It has been impractical, for example, to acquire observations of plant community successional stage at the regional level and over periods of decades or longer. The historic base of satellite remote sensing data and remote sensing technology opens the way for new model development, unconstrained by many of the limitations of ground based data collection methods.

In our research at the Goddard Space Flight Center, we are developing the use of satellite remote sensing to provide an additional tool for understanding the response of forested ecosystems to climate and other changes. We are using satellite remote sensing as a tool for the direct observation of forest dynamics as well as a tool to initialize and test forest dynamics models, *e.g.*, the FORET model of Shugart (1977). FORET as well as other models can be initialized by specifying species mix at the plot level using remote sensing data of some early vintage. The models can be run forward in time to predict a new state for the ecosystem and compared

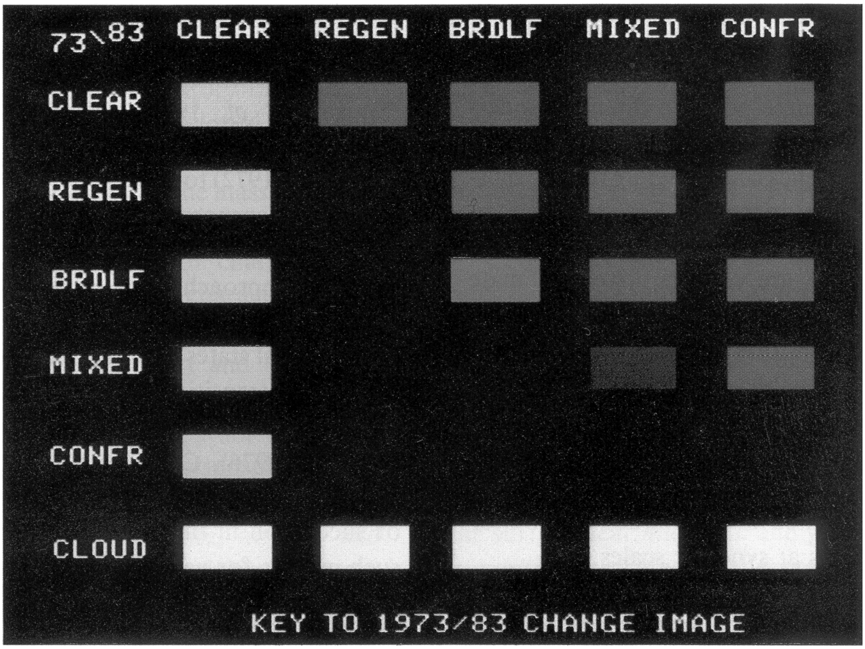

Fig. 3. Color-coded ecological state transition matrix and 10-year (1973–1983) ecological state transition map as generated from LANDSAT MSS data for a portion of the study area. This color matrix and resulting map emphasizes (1) landscape units that were vegetated in 1973, subsequently deforested and remained cleared in 1983 (yellow) and (2) landscape units supporting vegetative regrowth from 1973 clearings (red). Colors for unchanged landscape units are shown on the color matrix diagonals; Regressive disturbance transitions (purple) are shown on the lower, internal off-diagonals; Ecological succession (salmon) are shown on the upper, internal off-diagonals. Black boundaries distinguish the Boundary Waters Canoe Area protected wilderness (upper and lower portions of scene) from non-wilderness areas. White represents areas classified as clouds. Black represents areas classified as lakes and cloud shadows. Color assignments may be varied to aid the visual study of ecological succession patterns.

again to actual satellite observations of ecosystem status.

Multi-year sequences of remote sensing data can also be used to provide estimates of transition frequencies between ecological states, which can be used as inputs for Markov models of succession in the ecosystem. Practical difficulties include workable definitions of spectrally separable states and measuring (rather than inferring) actual transition probabilities (Lippe *et al.* 1985). Defining ecological states involves both finding an appropriate ecological parameter and breaking the continuum it represents into discrete pieces. In constructing Markov models, forest states have been most often classified on the basis of the species of canopy tree (Horn 1975a, b, 1976) or the most abundant species (Waggoner and Stephens 1970). A significant problem with such studies has been the effort (number of samples) required to obtain good estimates of the transition probabilities (model parameters), the number of which increases with the square of the number of states. A set of states which gives high ecological resolution can therefore require a prohibitive ground sampling effort. However, given a reliable satellite image processing approach, large areas can be exhaustively sampled by remote sensing. The choice of ecological states is limited only by the ability to discriminate and identify them with the remotely sensed spectral data. The frequency of state changes from year to year can then be determined by simple enumeration. The number of pixels in a typical image is so large that even rare state transitions are determined with reasonable precision.

In utilizing remote sensing data as input to both computer simulation and stochastic forest dynamics models, we begin by defining the states of forest landscape units based on age structure and species composition which are also observable from remote sensing data. The age structure and species compo-

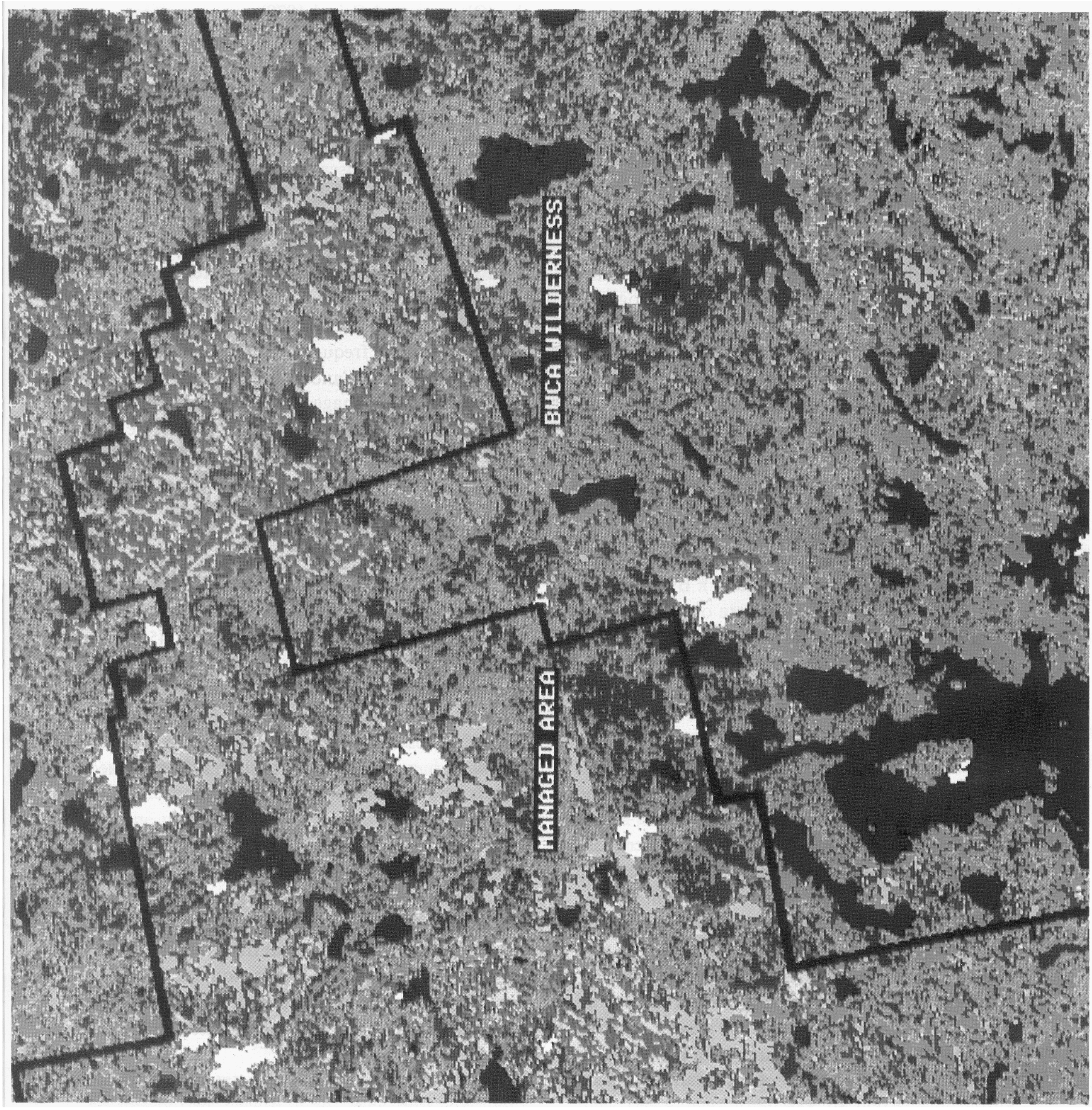

Fig. 3.

Table 1. Spectrally distinct ecological states, listed in order of average age since disturbance (youngest to oldest).

State	Description
Clearing	sparse or low density vegetation
Regeneration	predominantly young aspen & jack pine
Aspen	predominantly aspen/broadleaf species
Mixed	mixtures of conifers and broadleafs
Conifer	predominantly conifer species

sition are then associated with successional states using knowledge of the region and its ecology.

We have used remote sensing to study succession in the boreal forest of northern Minnesota. In this area, there is a managed forest (the Superior National Forest) and a wilderness area (the Boundary Waters Canoe Area) where the effects of human activities can be separated from other effects. There are two typical successional sequences (Grigal and Ohmann 1975); (i) clearing to regeneration to broadleaf to mixed broadleaf/conifer to conifer classes and (ii) clearing to regeneration to conifers (primarily jack pine, spurce and fir). By examining satellite and aircraft spectral data obtained during 1983 over sample plots in these successional stages we were able to determine that Landsat multispectral scanner data could be used to classify each landscape element (pixel) into one of the states in Table 1. By acquiring Landsat data from 1973 over the boreal forest, we were able to use the 1983 Landsat derived relationships between spectra and successional stage, correcting for inter-sensor calibration and inter-date atmospheric differences, to infer the successional state of the landscape in 1973.

Figure 3 is a color-coded transition map indicating successional transitions during the 10-year period. Color assignments are shown in the accompanying color transition matrix. Disturbance transitions to clearings (yellow) and regrowth from clearings (red) are widely scattered in the protected wilderness area. Almost all of the disturbance transitions to clearings are a result of logging and occur in the managed area. The extensive area of regrowth from clearings occurring in the upper right center of the transition image is associated with the 1971 Little Sioux forest fire which consumed 6,000 ha (Ohmann and Grigal 1979).

From the transition maps we can calculate the ecological state transition matrices (Tables 2A and B) which are direct measures of rates of change among successional states. Each diagonal element of a matrix is a ***retention frequency, i.e.***, the proportion of landscape elements in one state which remained in or has returned to the same state between 1973 and 1983. Each off-diagonal element is a ***transition frequency, i.e.***, the rate at which units in a given state change to other states during the 10-year period. Retention frequencies are indicative of stability, while ecological dynamics are captured in the transition frequencies. The transition matrices of Tables 2A and B indicate that both the wilderness and managed forest were highly dynamic at the landscape unit level; even the late successional classes had a retention frequency of less than 60%. The retention frequency of an ecological state increased with time since disturbance, with clearings having the lowest retention frequency. This is consistent with the slower turnover expected in late successional states (West ***et*** *al.* 1981). The highest between-state transition frequencies were for clearings to regeneration, exceeding 45%, the lowest from aspen to conifer, about 4%. This trend is consistent with expected successional trends. In contrast, disturbance transitions (from later to earlier successional states) were generally low for the wilderness (area; the transitions from mixed stands and from conifers to clearings were both about 1%.

Comparison of transition frequencies inside and outside of the protected wilderness provides a quantitative measure of the effects of recent human activities in the Superior National Forest. Disturbances, indicated by transitions from mature forested types to clearing and regeneration, are five to 10 times higher in the managed area than in the protected wilderness and are concentrated in logged areas.

Any system which is in a high state of flux at the landscape unit level for a 10-year period can be highly dynamic at a regional level over longer time periods. Recent perturbations to the system, such as fire suppression, increased logging and climate change could be rapidly affecting the composition

Table 2. Transition matries for the wilderness and managed portions of the study area. Matrix row and column labels are the ecological states of the forest as determined from remote sensing. Each element in the matrix is the calculated state transition frequency for the Landsat scene (100 X the number of scene pixels undergoing transition from the 1973 state to the 1983 state/total number of scene pixels). Diagonal elements are retention frequencies; off diagonal elements are transition frequencies. The category ***other*** includes unclassified, water, clouds and cloud shadows.

A. For an area of 534 km‘, with 148,406 landscape elements in the protected wilderness of the Boundary Waters Canoe Area.

B. For an area of 409 km², with 113,738 landscape elements in the multi-use Superior National Forest adjacent to the Boundary Waters Canoe Area.

A. Wilderness

1973 \ 1983	Clearings	Regenerating	Aspen	Mixed	Conifer	Other
Clearing	17.1	45.6	16.7	15.2	5.22	0.12
Regeneration	4.55	30.5	16.9	37.3	10.0	0.36
Aspen	1.12	19.7	47.1	27.6	4.16	0.28
Mixed	0.52	6.81	11.28	58.1	22.6	0.72
Conifer	1.04	4.37	1.81	31.0	57.8	3.93
Other	0.53	3.14	3.19	8.60	13.4	71.1

B. Managed

1973 \ 1983	Clearings	Regenerating	Aspen	Mixed	Conifer	Other
Clearing	20.7	47.1	9.97	17.8	4.64	0.12
Regeneration	8.18	36.4	13.7	32.7	8.84	0.14
Aspen	5.74	26.7	34.4	28.7	4.33	0.12
Mixed	5.89	13.5	8.19	51.1	21.0	0.31
Conifer	5.65	10.3	1.79	26.7	53.9	1.66
Other	3.36	16.6	12.9	23.9	16.2	26.9

of the boreal forest. The accumulated effects of such perturbations should be reflected in the observed elements of the transition matrices.

The transition matrix τ constitutes a model of forest dynamics. We can use the transition matrix to project into the future, the areal proportions of the landscape occupied by the observed successional stages. By successive multiplication with the current areal proportions p, we can project the future state of areal proportions ρ_m after m observation periods, *i.e.*,

$$\rho_m = \tau^m \rho_o \tag{11}$$

If we hold the transition matrix elements constant over time, we assume that climate and other changes have no effect on the transition rates and can project the steady state condition of the forest given an invariate climate by solving the eigenvector equation,

$$p = \tau \rho \tag{12}$$

In general the community composition approaches an equilibrium, or steady state. This steady state need not be the classic ‘climax community’; transitions to and from a ‘disturbance’ state can be included in the formalism. The frequency of such disturbances determines the nature of the steady state.

Using τ calculated from our analysis Table 3 gives the projected steady-state values of these proportions in both the wilderness and managed areas of the northern Minnesota study area. Even though individual landscape units have a high rate of change, current regional level areal proportions of ecological states are not greatly different from the projected future values. This is true for both the managed and wilderness areas even though rates of anthropogenic disturbances are very different for

Table 3. 1983 and projected future values of areal percentages occupied by ecological states.

Class	Wilderness		Managed	
	1983 (%)	Proj (%)	1983 (%)	Proj (%)
Conifer	23.1	27.2	20.9	22.2
Mixed CON/BL	35.8	39.3	34.5	35.2
Regeneration	11.9	10.3	21.6	20.9
Aspen	15.8	13.2	13.2	10.6
Clearings	1.7	1.3	7.2	7.2

the two regions. This result suggests that if currently observed rates of change at the landscape unit level persist, regional stability in the composition of the study area will be maintained.

Since the satellite data record is short compared to the time scales over which forested ecosystems respond to climate change, a transition matrix based on that satellite record cannot incorporate long-term climate trends. However, information or theories about how the transition matrix elements do change over time could in principle be incorporated *to* generate a climate dependent transition matrix describing forest dynamics. For example, we could use computer simulation models of growth and succession) to calculate transition rates as a function of climate variables (primarily moisture, light and temperature), and project future states as a function of assumed climate scenarios, *e.g.*, gradually increasing temperature and precipitation.

Alternatively, direct observations of τ over a climate gradient in space could be used to calculate τ as a function of climate increment in time. The climate dependent τ could then be used in (11) to project the forest structure in incremental steps as a function of climate scenario, thus trading space for time to understand the long-term response of the biosphere to climate. This would require the implementation of a gradient experiment, over some transect through a biome whose community composition and structure varies with climate.

Such transects are known to exist. An example is shown in Fig. 4 from Glaser (1987). Exhibit 4 of Fig. 4, a map of the presettlement vegetation of Minnesota, shows a gradation in community com-

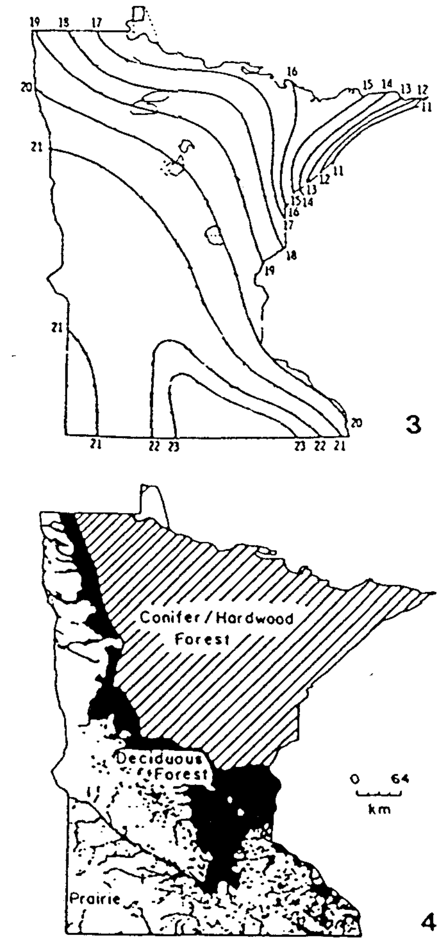

Fig. 4. Climate and vegetation of Minnesota from Glaser (1987). Exhibit 3 is average annual evapotranspiration in inches. Exhibit 4 is presettlement vegetation of Minnesota.

postion and structure from southwest to northeast across the state. Exhibit **3** shows a corresponding map of the annual evapotranspiration based on climatological data (moisture and temperature) as calculated from the Thornwaite method. The community composition and structure closely follows the evapotranspiration isopleths. In particular, the deciduous forest is confined in a very narrow range at the 22” isopleth. A sample of multi-year Landsat data across **a** transect perpendicular to the evapotranspiration isopleths could be used to calculate the transition matrices as a function of the annual evapotranspiration rate. From atmospheric general circulation models then, various climate scenarios could be generated, for example as a function of in-

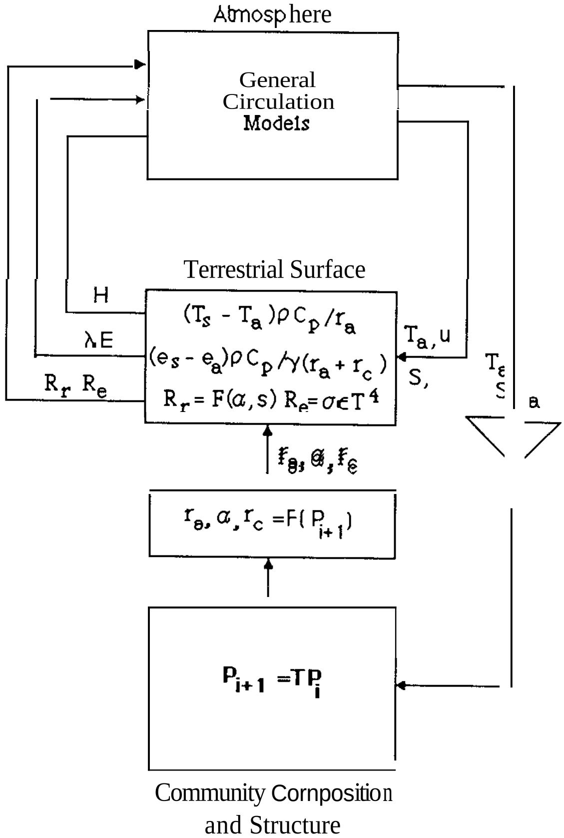

Fig. **5.** Simplified interation diagram of biosphere/atmosphere showing coupling at two different temporal scales between a vegetated landscape and the atmosphere.

creasing atmospheric CO_2. Previous experience with these simulations show that temperature will increase over time and thus evapotranspiration. The rate of increase in evapotranspiration with time could then be used to calculate a sequence of expected transition matrices as a function of time. This sequence of transition matrices could then be used in (12) to examine the forest dynamics as a function of changing climate.

Feedback between the biosphere and the atmosphere

To examine some parameters involved in feedback between the biosphere and the atmosphere, we can now turn to Fig. 5, which represents a simple biosphere/atmosphere interaction model, with feedback, assuming a planet whose entire surface is composed of vegetation. While such a model is of course not realistic it will hopefully illustrate in some more detail the notions we have been discussing. **As** we mentioned earlier the partitioning of the radiation by the surface soil and vegetation into sensible heat, latent heat, visible and thermal radiation can significantly affect the atmospheric fields of radiation, temperature, moisture and precipitation over the continents. The relations **(1)**, **(2)**, **(3)** and **(4)** relate the atmospheric state T,, e, **S,** and u (windspeed), to the fluxes of H, and XE returned from the terrestrial surface back to the atmosphere. Over the longer time scales we can allow the community composition and structure of the terrestrial vegetation to modulate the biophysical parameters of the vegetation. For example, if we use the output of the general circulation models, to calculate temperature and precipitation fields, we can compute evapotranspiration as a function of time. These evapotranspiration rates can in turn be used to calculate τ as a function of time and project community composition and structure as in (11). ρ in turn specifies an average vegetative structure, such as height, leaf area and leaf reflectance and can be related to the canopy aerodynamic resistance, r_a, the photosynthetic capacity, r_c, and the albedo of the vegetation α.

Obviously, this is a very general scenario, and many details would need to be worked out in order to actually implement such a study. But it points out the desireability of simultaneously investigating the biosphere to atmosphere interactions and the climate to biosphere interactions.

Conclusions

We have argued the importance and feasibility of developing coupled models, expressing the interactions between the biosphere-climate system. In the context of such models, remote sensing potentially plays a critical role. First, remote sensing techniques can be used to infer many of the parameters required as inputs to the coupled biosphere-atmosphere models: inputs such as surface temperature, evapotranspiration rate, solar radiation interception, photosynthetic capacity, soil moisture, aerodynamic and surface resistance of the vegetation. These parameters along with surface-measured and satellite-inferred meteorological data can be used to determine a vegetation-dependent surface energy budget, a necessary input to global circulation models. Secondly, because remote sensing techniques allow us to measure these parameters at a wide range of temporal and spatial scales, the use of such techniques can help us transfer our understanding of biological-atmosphere processes at a small scale up regional continental and global scales. Finally, remote sensing techniques can be used to map and monitor the ecological state of terrestrial ecosystems, *e.g.*, successional state, community composition and structure, net primary productivity, and the time rate of change of these ecosystems.

It should be noted that our arguments did not consider many of the important interactions coupling the biosphere to the atmosphere, for example the role of chemical cycling and the important effect of trace gases on atmospheric composition and future climate, or the effect of atmospheric pollutants on the community composition and structure of terrestrial ecosystems. These areas are beyond our spheres of expertise but certainly they must be considered in any model linking the biosphere to the atmosphere/climate system. We believe, however, the efforts we did discuss point up the need and the direction for future work.

It is our expectation that FIFE will support many of the hypotheses we have stated herein, at least for the simple prairie grassland which served as the initial testing ground. A logical step is to move beyond the prairie test bed to other biomes. We must also move beyond the local level of FIFE to regional levels where coupled land surface/atmosphere models can be tested. In addition we must include studies of the biogeochemical cycles, their effects on atmospheric composition and climate and the use of remotely sensed data to monitor the biochemical status of vegetated ecosystems. As we have shown, the effect of climate, biogeochemical and hydrological cycles and anthropogenic effects on the composition and structure of terrestrial landscapes must be an important component of these efforts. These effects are complex; therefore, we must in the very near term extend our research and experimentation of plot-level climate effects to the regional and global levels.

How can we accomplish these things with limited people and resources? It is our belief that we must concentrate initially on a single biome, using sites distributed along an important environmental gradient. Spatial variation can then permit us to trade space for time in understanding the long-term effects of these environmental gradients on ecosystems. Within this framework, a multi-disciplinary effort should be mounted to examine all the major aspects of the biosphere/atmosphere coupling. FIFE demonstrated that such an interdisciplinary effort is manageable and that the synergistic effects between disciplines are considerable.

References

Asrar, G. and Kanemasu, E.T. **1986.** Estimating regional evapotranspiration from remotely sensed data by surface energy balance models, Kansas Evapotranspiration Laboratory, Manhattan, Kansas, Final Report on Grant NAG 5-389.

Arakawa, A. and Suarez, M.J. **1983.** Vertical differencing of the primitive equations in sigma coordinates. Mon Weath Rev. **111: 34–45.**

Becker, F.B., Camillo, P.J. and Choudhury, B.J. (in prep.) The surface energy balance, (available from P.J. Sellers, code **624,** Goddard Space Flight Center, Greenbelt Md., **20771).**

Bormann, **F.H.** and Likens, G.E. **1979.** Pattern and process in a forested ecosystem. Springer-Verlag, New York.

Botkin, D.B., Janak, J.F. and Wallis, J.R. **1972.** Some ecological consequences of a computer model of forest growth. J. Ecol. **60: 849–872.**

Carson, D.J. 1981. Current parameterization of land surface processes in atmospheric General Circulation Models. *In* Proceedings JSC Study Conference Land-Surface Processes in Atmosphere General Circulation Models. Edited by P.S. Eagleton. pp. **67–108.**

Carson, D.J. and Sangster, A.B. **1981.** The influence of land-surface albedo and soil moisture on general circulation model simulations. Numerical Experimentation Programme Report No. **2:**5.14–5.21.

Charney, J.G., Quirk, W.J., Chow, S.H. and Kornfield, J. **1977.** A comparative study of the effects of albedo change in semi-arid regions. J Atmos. Sci. **34: 1366–1385.**

Chervin, R.M. **1979.** Response of the NCAR general circulation model to changed land surface albedo. Report of the JOC study conference on climate models: Performance, intercomparison and sensitivity studies, Vol. 1: **563–581.**

Deardorff, J.W. **1977.** Efficient prediction of ground surface temperature and moisture, with inclusion of a layer of vegetation. J. Geophy Res. 83: 1889–1903.

Dobson, M.C. and Ulaby, F.T. 1986. Active microwave soil moisture research, IEEE Trans Geosci. and Rem. Sens. GE-24(1): 23–26.

Dickinson, R.E. 1984. Modeling evapotranspiration for three-dimensional global climate models. Climate Processes and Climate Sensitivity: Am. Geophys. Union Monogr. 29: 58–72.

Emanuel, W.R., Shugart, H.H. and Stevenson, M.P. 1985. Climatic change and the broad-scale distribution of terrestrial ecosystem complexes. Climatic Change 7: 29–43.

Farquhar, G.D. and Sharkey, T.D. 1982. Stomatal conductance and photosynthesis. Ann. Rev. Plant Physiol. 33: 317–345.

Fung, A.K. and Eom, H.J. 1981. An approximate model for backscattering and emission from land and sea, IEEE Int. Geos. and Rem. Sens. Symposium, 1: 620–628.

Grigal, D.F. and Ohmann, L.F. 1975. Classification, description and dynamics of upland plant communities within a Minnesota wilderness area. Ecol. Monogr. 45: 389–407.

Glaser, P.H. 1987. The ecology of patterened boreal peatlands of northern Minnesota: A community profile. Fish and Wildl. Serv. Rep. 85(7.14).

Hall, F.G., Strebel, D.E., Goetz, S.J., Woods, K.D. and Botkin, D.B. 1987. Landscape pattern and successional dynamics in the boreal forest. Proceedings of the 1987 IGARRS Symposium, IEEE87CH2434-9:473–483.

Hope, A.S. 1987. Parameterization of surface moisture availability for evapotranspiration using combined remotely sensed spectral reflectance and thermal observations, PhD thesis, RSSL, University of Maryland, College Park MD, 20742.

Horn, H.S. 1975a. Forest succession. Scient. Am. 232(5): 90–98.

Horn, H.S. 1975b. Markovian properties of forest succession. *In* Ecology and Evolution of Communities. Edited by M.L. Cody and J.M. Diamond. pp. 196–211.

Horn, H.S. 1976. Forest succession in theoretical ecology. Saunders, Philadelphia.

Hulst, R.V. 1979. On the dynamics of vegetation: Markov chains as models of succession. Vegetatio 40: 3–14.

Kauth, R.J. and Thomas, G.S. 1976. The tasselled cap, a graphic description of the spectral-temporal development of agricultural crops as seen by Landsat. Proceedings 3rd Symposium Machine Processing of Remotely Sensed Data, Purdue. University, IEEE 76 CH 1103-1: 4B-41-4B-51.

Lippe, E., De Smidt, J.T. and Glenn-Lewin, D.C. 1985. Markov models and succession: A test from a heathland in the Netherlands. J. Ecol. 73: 775–791.

MacCracken, M.C. and Luther, F.M. 1985. Projecting the climatic effects of increasing carbon dioxide, U.S. Department of Energy, Washington D.C., DOE/ER-0237:381.

Matthews, E. 1983. Global vegetation and land use: New high resolution data bases for climate studies. J. Clim. Appl. Meteor. 22: 474–487.

McNaughton, K.G. and Spriggs, T.W. 1986. A mixed-layer model for regional evaporation. Bound. Layer Meteor. 37: 243–262.

Mintz, Y. 1984. The sensitivity of numerically simulated climates to land-surface conditions. *In* The Global Climate. Edited by J. Houghton. pp. 79–105.

Miyakoda, K. and Sirutis, J. 1986. Manual of E-physics. Manuscript, GFDL, Princeton.

Mo, T., Schmmugge, T.J. and Jackson, T.J. 1984. Calculations of radar backscattering coefficient of vegetation-covered soils. Rem. Sens. of Environ. 15: 119–133.

Monteith, J.L. 1973. Principles of environmental physics. Edward Arnold, London.

Ohmann, L.F. and Grigal, D.F. 1979. Early revegetation and nutrients dynamics following the 1971 Little Sioux Forest Fire in Northeastern Minnesota. Supplement to Forest Science Vol. 25 no. 4, Dec. 1979.

Orszag, S.A. 1970. Transform methods for calculation of vector coupled sums: Applications to the spectral form of the vorticity equations. J. Atmos. Sci. 27: 870–895.

Pitts, D.E., Badhwar, G. and Reyna, E., Zoughi, R. and Wu, L.K. 1988. Estimation of X band scattering properties of tree components, IEEE Trans. Geos. and Rem. Sens. (in press).

Pitts, D.E., Badhwar, G. and Reyna E. 1987. Estimation of biophysical properties of forest canopies using C-band. Adv. in Space Res. 7(11): 89–95

Revelle, R. and Munk, W. 1977. The carbon dioxide cycle and the biosphere. National Academy of Sciences, Wash. DC. pp. 140–158.

Salati, E. and Vose, P.B. 1984. Amazon Basins. A system in equilibrium. Science 225: 129–138.

Schmugge, T.J. 1983. Remote sensing of Soil Moisture: Recent Advances, IEEE Trans. Geoscience and Rem. Sensing GE-21 3: 336– 344.

Schmugge, T. and Sellers, P.J. 1986. FIFE Science Plan. Internal NASA Document, Earth Resources Branch-code 623, NASA Goddard Spaceflight Center.

Sela, J.G. 1980. Spectral modeling at the National Meteorological Center. Mon. Weath. Rev. 108(9): 1279–1292.

Sellers, P.J. 1985. Canopy reflectance photosynthesis and transpiration. Int. J. Rem. Sens. 8(6): 1335–1372.

Sellers, P.J., Mintz, Y., Sud, Y.C. and Dalcher, A. 1986. A simple biosphere model (SiB) for use within general circulation models. J. of Atmos. Sci. 43(6): 505–531.

Sellers, P.J. 1987. Canopy reflectance, photosynthesis and transpiration II: the role of biophysics in the linearity of their interdependence. Rem. Sens. Env 21: 143–183.

Sellers, P.J. and Dorman, J.L. 1987. Testing the simple biosphere model (SiB) with point micrometeorological and biophysical data. J. Clim. and Appl. Meteor. 26(5): 622–651.

Sellers, P.J. and Hall, F.G. 1987. FIFE Experiment Plan, Internal NASA Document, Earth Resources Branch-code 623, NASA Goddard Spaceflight Center.

Sellers, P.J., Hall, F.G., Asrar, G., Strebel, D.E. and Murphy, R.E. 1988. The First ISLSCP Field Experiment (FIFE). Bull. of Amer. Met. Soc. 69(1): 22–27.

Sellers, P.J. and Rasool, S.I. (in prep.) Report on a workshop on satellite data algorithms, (available from P.J. Sellers, code 624, NASA/GSFC, Greenbelt Md).

Shugart, H.H., Crow, T.R. and Hett, J.M. 1973. Forest succession models: a rationale and methodology for modeling forest succession over large regions. For. Sci. 19: 203–212.

Shugart, H.H. and West, D.C. 1980. Forest succession models. BioScience 30: 308–313.

Shugart, H.H. 1984. A theory of forest dynamics. Springer-Verlag, New York.

Shukla, J. and Mintz, Y. 1982. Influence of land-surface evapotranspiration on the earth's climate. Science 215: 1498–1501.

Solomon, A.M. and Webb III, T. 1985. Computer-aided reconstruction of late-Quaternary landscape dynamics. Ann. Rev. Ecol. and System. 16: 63–84.

Sud, Y.C. and Fennessy, M. 1982. A study of the influence of surface albedo on July circulation in semi-arid regions using the GLAS GCM. J. Clim 2: 105–125.

Sud, Y.C. and Smith, W.E. 1985. The influence of surface roughness of deserts on the July circulation. Boundary Layer Met. 33: 15–49.

Shuttleworth, W.J. et al. 1984a. Eddy correlation measurements of energy partition for Amazonian forests. Quart. J. Roy. Met. Soc. 110: 143–1163.

Shuttleworth, W.J. et al. 1984b. Observations of radiation exchange above and below Amazonian forests. Quart. J. Roy. Met. Soc. 110: 1163–1169.

Tsang, L., Blanchard, A.J., Newton, R.W. and Kong, J.A. 1982. A single relation between active and passive microwave remote sensing measurements of earth terrain, IEEE Trans. Geos. Rem. Sens. GE-20(4): 482–485.

Ulaby, F.T., Aslam, A. and Dobson, M.C. 1982. Effects of vegetation cover on the radar sensitivity to soil moisture, 1982. IEEE Trans. Geos. and Rem. Sens. GE20(4): 476–481.

Usher, M.B. 1981. Modelling ecological succession, with particular reference to Markovian models. Vegetatio 46: 11–18.

Walker, J.M. and Rowntree, P.R. 1977. The effect of soil moisture on circulation and rainfall in a tropical model. Quart. J. Roy. Meteor. Soc. 103: 29–46.

Waggoner, P.E. and Stephens, G.R. 1970. Transition probabilities for a forest. Nature 225: 1160–1161.

Warrilow, D.A. 1986. The sensitivity of the UK Meteorological Office atmospheric general circulation model to recent changes in the parameterization of hydrology, ISLSCP, Proc. of an International Conference in Rome, Italy, December 1985, ESA SP-248, European Space Agency, Paris, France: 143–150.

West, D.C., Shugart, H.H. and Botkins, D.B. (eds). 1981. Succession: concepts and applications. Springer-Verlag, New York.

Wiin-Nielsen, A. 1976. Atmospheric predictability on various scales. Naturwissenschaften 63: 506–512.